

Interference Rejection using the Data-Recycling Algorithm in DS Spread-Spectrum Communications

Nam Yong Kim

Abstract

In this paper, a new interference rejection filter using the data-recycling technique is presented. The reference signal of the interference rejection filter is formed by using chip decisions, which is correlated with the narrowband interference components of the received signal. The decision feedback techniques reduce the distortion of the desired signal, which is introduced by the interference rejection filter through the use of feedback chip decisions. In order to update the filter coefficients a simple and efficient data-recycling technique that has improved performance over the conventional LMS algorithm is used. The performance of the proposed interference rejection filter is compared to filters with conventional LMS linear filter. The results show that the convergence speed of the proposed interference rejection filter using decision feedback and data-recycling technique is significantly faster than that of the conventional filters. Also, BER performance of the interference rejection filter demonstrates the superiority of the proposed filter algorithm.

I. Introduction

DS spread spectrum communication system has an ability to suppress interference as much as its processing gain. In general, it is necessary to increase the processing gain in order to get better performance in the presence of interference power. But additional processing gain is obtained at the expense of larger transmit bandwidth or reduced data rate. The goal of an interference rejection filter is to provide greater tolerance to interferences without increasing the processing gain. To enhance the performance of conventional systems, digital filtering techniques can be employed prior to correlation [1].

Adaptive filters have been used in many applications including narrowband jamming rejection [2] [3] [4]. The jamming rejection properties of a receiver using an adaptive filter can be improved by making use of the correlation properties of spread spectrum signals and narrowband interferences.

It is demonstrated by [5] that the use of decision feedback filters offers improved performance over linear techniques. In

this paper, a new data-recycling LMS algorithm [6] using decision feedback (DF) for estimating and suppressing the narrowband interference is presented.

One of the convergence characteristics of the data-recycling algorithm, in which the coefficients are multiply adapted in a symbol time period by recycling the received data, is that the data-recycling technique can increase convergence speed by $(B+1)$ times, where B is the number of recycled data [6].

The performance of the proposed interference canceller, which uses the decision feedback technique, is compared to the linear (Non-DF) interference cancellation filter structure.

It is assumed that the processing gain is fixed as 7 and signal to interference ratio is -10 [dB] in the simulation.

This paper is composed of 5 sections. The first section serves as the introduction. In section 2, decision feedback interference rejection filter structure is introduced. Data-recycling LMS algorithm for interference rejection filter is presented in section 3. In section 4, we demonstrate the superiority of the proposed filter in a computer simulation for narrow band interference rejection. Finally, conclusions are given in section 5 and references are given thereafter.

II. Decision Feedback Interference Rejection Filter Structure

Manuscript received September 12, 1997; accepted December 26, 1997.

N. Y. Kim is with the Dept. of Informations & Communications Engineering, Samchok National University.

A Decision feedback interference rejection filter structure is shown in Figure 1. $r(k)$ is the sampled output of the chip pulse matched filter, consisting in general of a desired signal component $d(k)$, a white Gaussian noise component $n(k)$, and a narrowband interference component $i(k)$:

$$r(k) = d(k) + n(k) + i(k) \tag{1}$$

The PN chip code for spreading is $p(k)$.

It can be seen that if a reference signal, $x(k)$, correlated with the narrowband interference component of the received signal, is available, the interference component in the received signal can be estimated and subtracted out as shown in Figure 1.

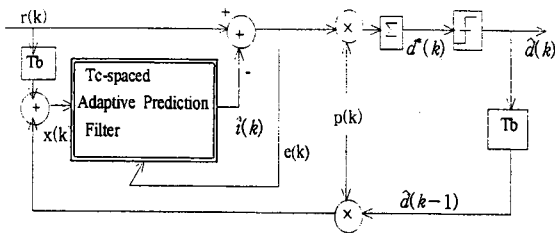


Fig. 1. Decision feedback interference suppressor with adaptive predictor.

A temporary decision $\hat{d}(k)$ can be subtracted from the received signal as shown in Figure 1. The interference reference described above is given by:

$$x(k) = r(k-1) - \hat{d}(k-1) \tag{2}$$

which yields an interference estimate given by:

$$\hat{i}(k) = \sum_{j=0}^L c_j(k) x(k-j) \tag{3}$$

and the estimate of the transmitted sequence given by:

$$d^*(k) = r(k) - \hat{i}(k) = r(k) - \sum_{j=0}^L c_j(k) r(k-1-j) + \sum_{j=0}^L c_j(k) \hat{d}(k-1-j) \tag{4}$$

The filter coefficients, $c_j(k)$, may be found by solving the set of $L+1$ linear equations

$$R(n) = \sum_{k=0}^L c_j(k) [R(n-k) - \sigma_d^2 \delta_{k,n}] \tag{5}$$

where $n=0,1,2,\dots,L$, σ_d^2 is the variance of $d(k)$ and Kronecker $\delta_{k,n} = 1$ for $n=k$. The chip decision, $\hat{d}(k)$, which is used to make $x(k)$, can be formed in several ways. The most straightforward way is simply to employ a threshold and decide $\hat{d}(k) = 1$ if $d^*(k) > 0$, and $\hat{d}(k) = -1$ if $d^*(k) < 0$. As described earlier, the adaptive predictor cannot accurately estimate the DS code sequence and, therefore, tends to estimate only the narrowband jamming. This error residual, which represents the difference between the current input sample and its estimate based on L previous samples, where

L is the filter order, is the portion of the input signal which the adaptive filter cannot estimate, i.e., the DS code. The effect of the decision feedback canceller, when decisions are fed back, is to estimate the interference with undistorted delayed interference. The reference input of the predictor is the pure jamming signal, which is the subtracted residual. Because the input of the filter is not distorted by DS code, the predictor can estimate more effectively the interference components.

III. The Data-Recycling LMS Algorithm

Consider the data-recycling filter structure in Figure 2 which is used as the predictor depicted in Figure 1.

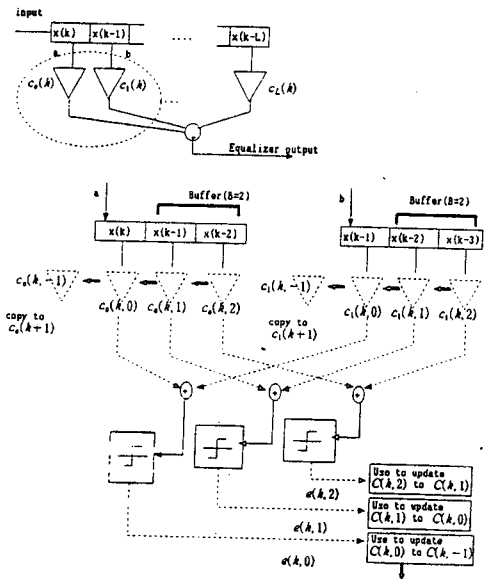


Fig. 2. The data-recycling algorithm.

The filter output $\hat{i}(k)$ is given by the following equation with input signal vector $X(k)$ and coefficient vector $C(k)$.

$$\hat{i}(k) = \sum_{j=0}^L c_j(k) \cdot x(k-j) \tag{6}$$

The error signal can be expressed as the difference between desired signal $r(k)$ and filter output $\hat{i}(k)$ as $e(k) = r(k) - \hat{i}(k)$. Then the LMS algorithm is expressed in the following form[6].

$$C(k+1) = C(k) - \mu \cdot \left(\frac{\partial e^2(k)}{\partial C(k)} \right) = C(k) + 2\mu \cdot e(k) \cdot X(k) \tag{7}$$

Where $C(k) = [c_0(k), c_1(k), \dots, c_L(k)]^T$ and $X(k) = [x(k), x(k-1), \dots, x(k-L)]^T$.

In the simulation described in section IV, this LMS

algorithm is applied to the DF interference suppressor depicted in Figure 1.

Instead of using a single $X(k)$ to update the coefficient, we can use the discarded data vectors ($X(k-1)$, $X(k-2)$, $X(k-3)$. . .) which are stored in some finite buffers. The structure with the buffers used for recycling data and the coefficient-updating process are depicted in the lower part of Figure 2. The flow chart for updating $C(k)$ is shown in Figure 3.

For simplicity, the proposed structure including just two taps **a** and **b** is described. Tap **a** and **b** have two recycling data ($B=2$) in their buffers each. Firstly, the recycling data $X(k-2)$ in the buffer of tap **a** and $X(k-3)$ in the buffer of tap **b** are used to update $C(k,2) = [c_o(k,2), c_1(k,2)]^T$ to $C(k,1) = [c_o(k,1), c_1(k,1)]^T$ using error $e(k,2)$. Secondly, $C(k,1) = [c_o(k,1), c_1(k,1)]^T$ is updated to $C(k,0) = [c_o(k,0), c_1(k,0)]^T$ using $X(k-1) = [x(k-1), x(k-2)]^T$ and $e(k,1)$. Finally, the data vector $X(k-0) = [x(k-0), x(k-1)]^T$ and coefficient vector $C(k,0) = [c_o(k,0), c_1(k,0)]^T$ produce $e(k,0)$. Now, $C(k,-1)$ is copied to the TDL filter coefficient vector $C(k+1)$, which will be used to produce $\hat{y}(k+1)$.

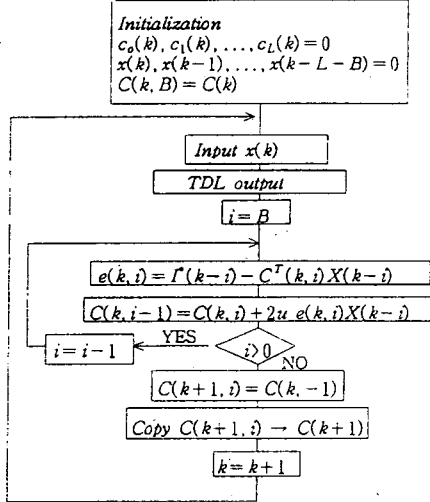


Fig. 3. The flow chart for updating $C(k)$.

The relationship between $C(k+1)$ and $C(k)$ from the flow chart in Figure 3 can be expressed as the following

$$C(k+1) = C(k) + 2u \sum_{i=0}^B e(k, i)X(k-i) \quad (8)$$

Using the equation $e(k, i) = I(k-i) - C^T(k, i)X(k-i)$ and taking the expected value of both sides of (8) yields

$$E[C(k+1)] = E[C(k)] + 2u \sum_{i=0}^B (E[I(k-i)X(k-i)] - E[X(k-i)X(k-i)^T]E[C(k, i)]) \quad (9)$$

In the equation (9) we have assumed that the input signal and tap coefficients are independent [7]. Letting R be defined as $R = E[XX^T]$ we can acquire the following equation(10).

$$E[C(k+1)] = E[C(k)] + 2u \sum_{i=0}^B (E[I(k-i)X(k-i)] - R \cdot E[C(k, i)]) \quad (10)$$

Assuming that R is nonsingular, the product of R and the optimal coefficient vector C^o is found to be equal to $E[I^T(k-i)X(k-i)]$. Thus

$$E[C(k+1)] = E[C(k)] + 2u \sum_{i=0}^B (RC^o - R E[C(k, i)])$$

or

$$E[C(k+1)] - C^o = (I - 2uR)(E[C(k)] - C^o) - 2u \sum_{i=1}^B R (E[C(k, i)] - C^o) \quad (11)$$

The equation (11) can be expressed more conveniently when we define a coefficient deviation vector $V(k, i) = E[C(k, i)] - C^o$, where its j th element is $v(k, i, j)$. When $i=0$, $C(k, 0)$ becomes $C(k)$ and $V(k, 0)$ becomes $V(k)$. Therefore, $E[C(k)] - C^o$ becomes $V(k)$ whose j th element is $v(k, 0, j)$. Thus

$$V(k+1) = (I - 2uR) V(k) - 2u \sum_{i=1}^B R V(k, i) \quad (12)$$

By the way, the input correlation matrix R can be expressed as the normal form $R = Q\Lambda Q^{-1}$, where Λ is the diagonal eigenvalue matrix and Q is the eigenvector matrix of R . We rotate $V(k)$ to the principal axes V' using $V' = Q^{-1}V$, so

$$V'(k+1) = Q^{-1}(I - 2uR)QV'(k) - 2u \sum_{i=1}^B Q^{-1}RQ V'(k, i) = (I - 2u\Lambda)V'(k) - 2u \sum_{i=1}^B \Lambda V'(k, i) \quad (13)$$

The j th element of $V'(k+1)$, $V'(k)$ and $V'(k, i)$ are, respectively, $v'(k+1, 0, j)$, $v'(k, 0, j)$ and $v'(k, i, j)$. Using these corresponding elements, (13) can be written as

$$v'(k+1, 0, j) = (1 - 2u\lambda_j) v'(k, 0, j) - 2u\lambda_j [v'(k, 1, j) + v'(k, 2, j) + \dots + v'(k, B, j)] = v'(k, 0, j) - 2u\lambda_j [v'(k, 0, j) + v'(k, 1, j) + v'(k, 2, j) + \dots + v'(k, B, j)] \quad (14)$$

The term $v'(k, B, j)$ becomes $v'(k, 0, j)$ by the iterations of the following equation.

$$v'(k, B-i, j) = (1 - 2u\lambda_j) v'(k, B-i+1, j) \quad (15)$$

The equation (15) with geometric ratios $1 - 2u\lambda_j$, can be written as

$$v'(k+1, 0, j) = v'(k, 0, j) - 2u\lambda_j [v'(k, 0, j)(1 - (1 - 2u\lambda_j)^{B+1}) / (1 - (1 - 2u\lambda_j))] \quad (16)$$

or

$$v'(k+1, j) = v'(k, j) [1 - 2u\lambda_j (1 - (1 - 2u\lambda_j)^{B+1}) / (1 - (1 - 2u\lambda_j))] \quad (17)$$

Rearranging yields

$$v'(k+1, j) = v'(k, j) - 2u\lambda_j \left[\frac{v'(k, j)}{2u\lambda_j} - \frac{v'(k, j)}{2u\lambda_j} (1 - 2u\lambda_j)^{B+1} \right] = v'(k, j) (1 - 2u\lambda_j)^{B+1} \tag{18}$$

The equation (18) indicates that the distance between the current tap coefficients and the optimal coefficients decreases with these geometric ratios $(1 - 2u\lambda_j)^{B+1}$. Comparing to the geometric ratios for the LMS algorithm $1 - 2u\lambda_j$ [7], the MSE ratios of the proposed can be expressed as

$$MSE \text{ ratio} = (1 - 2u\lambda_j)^{2(B+1)} \tag{19}$$

also

$$\log (MSE \text{ ratio}) = (B+1) \log (1 - 2u\lambda_j)^2 \tag{20}$$

This indicates that the proposed has $(B+1)$ times improved convergence speed in comparison with the LMS algorithm.

IV. Computer Simulation Results and Discussions

A computer simulation was used to evaluate the performance of the linear and proposed structure for interference (jamming) suppression. Random data is modulated by a PN code and added to white Gaussian noise and a single tone or narrowband jammer. This composite signal is processed through the adaptive filter and then a correlator. The recovered data at the correlator output is compared with the actual transmit data to determine BER. The model that we use for narrowband interference consists of a sum of equally spaced sinusoids covering 5 percent of the signal band. In particular, for the sum of sinusoids model, $i(k)$ is expressed as

$$i(k) = \sum_{m=1}^Q A_m \cos(2\pi f_m k + \phi_m) \tag{21}$$

where the amplitudes $\{A_m\}$ were selected to be 1 and the phases are uniformly distributed on the interval $(0, 2\pi)$. For convenience sake, the case that the LMS algorithm (7) was used in the DF interference suppressor is called DF (LMS) and the case that it was used in the suppressor without $\hat{d}(k-1)$ is called linear (LMS). The number of tones used in our simulation is $Q = 100$ tones [2]. In addition, a white Gaussian noise sequence with various E_b/N_0 is added to the canceller input. For both structures and both algorithms, 16 taps are used and the convergence parameter μ is 0.00001. The MSE learning curves are displayed in Figure 4. The frequency response (Figure 5) also shows the superior performance of the filter of Data-Recycling LMS algorithm over that of the LMS with DF and without DF (linear). In Figure 6, BER performance is presented. Figure 4, 5 and 6

are results for PN sequences of 7 chips using the linear and the decision feedback filters. these curves are obtained with SIR=-10[dB].

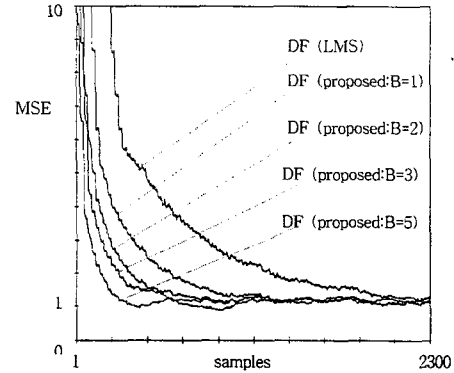


Fig. 4. MSE performance of the receiver with DF.

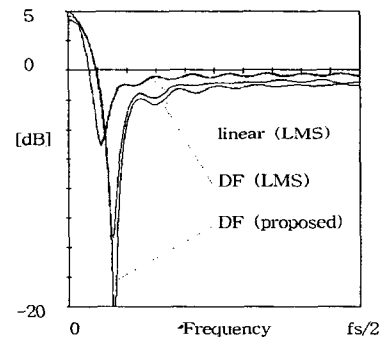


Fig. 5. Frequency response.

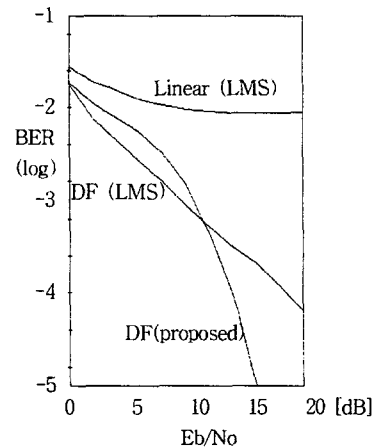


Fig. 6. BER performance of the receiver with and without DF.

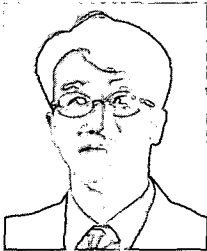
V. Conclusions

It was shown that the decision feedback technique can suppress the interference more efficiently when the data-recycling LMS algorithm is used for updating the filter coefficients. The theoretical analysis shows that the data-recycling LMS technique can increase convergence speed by $(B+1)$ times, where B is the number of recycled data. Curves for the linear structure show slower convergence than the DF structure in MSE. The BER performance of the proposed structure has about 3 dB improvement at $BER=0.0001$ in comparison with the linear system. These results indicate that the proposed structure is preferable for cases when fast converging adaptive filtering and excellent error performance are needed.

References

[1] Hsu, F. M., and Giordano, A. A. "Digital whitening techniques for improving spread spectrum communication performance in presence of narrowband jamming and interference," *IEEE Trans. commun.* vol. COM-26, pp.

- 209-216, Feb. 1978.
- [2] Ketchum, J. W. and Proakis, J. G., "Adaptive algorithms for estimating and suppressing narrowband interference in PN spread spectrum systems," *IEEE Trans. commun.* vol. COM-30, pp. 913-923, May, 1982.
- [3] Iltis, R. A., and Milstein, L. B., "An approximate statistical analysis of the Widrow LMS algorithm with application to narrowband interference rejection." *IEEE Trans. commun.* vol. COM-33, pp. 121-130, Feb. 1985.
- [4] Laurence B. Milstein and Ronald A. Iltis, "Signal processing for interference rejection in spread spectrum communications", *IEEE ASSP Magazine*, pp. 18-31, April, 1986.
- [5] J. W. Ketchum, "Decision feedback techniques for interference cancellation in PN spread spectrum communication systems," *IEEE military communication conf.*, pp. 39.5.1-39.5.5, Oct. 1984.
- [6] Nam Yong Kim, "Convergence Analysis of Data-Recycling LMS Equalizer", *The journal of Korean Institute of Communication Sciences*, vol. 21, No. 8, pp. 1905-1913, Aug. 1996.
- [7] B. Widrow, *Adaptive Signal Processing*, Prentice -Hall, 1985.



Nam-Yong Kim was born in Donghae, Korea in 1963. He received the B.S., M.S. and Ph. D from Yonsei University, all in electronic engineering in 1986, 1988 and 1991, respectively. From 1992 to 1997 he was in dept. of electronic communications engineering at Kwandong university. He is currently an

assistant professor of the Information & Communications engineering of Samchok national university, Samchok. His current research interests are signal processing in digital communications, satellite communications, mobile & personal communications.